(4)

ARL-STRUC-TM-568

AR-006-120

DEPARTMENT OF DEFENCE

DEFENCE SCIENCE AND TECHNOLOGY ORGANISATION

AERONAUTICAL RESEARCH LABORATORY

MELBOURNE, VICTORIA

AD-A227 755
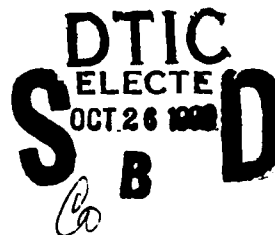
Aircraft Structures Technical Memorandum 568

VIBRATION OF A RECTANGULAR CANTILEVER PLATE

by

P.A. Farrell

and

T.G. Ryall

DTIC
ELECTE
OCT.26 1990
B
D

Approved for public release.

JULY 1990

90 10 2 083

AR-006-120

DEPARTMENT OF DEFENCE
DEFENCE SCIENCE AND TECHNOLOGY ORGANISATION
AERONAUTICAL RESEARCH LABORATORY

Aircraft Structures Technical Memorandum 568

VIBRATION OF A RECTANGULAR CANTILEVER PLATE

by

P.A. Farrell

and

T.G. Ryall

SUMMARY

In preparation for an experimental evaluation of the photogrammetry technique for measuring vibration mode shapes, a cantilever steel plate was designed. This report describes the theoretical methods used to calculate the low order natural frequencies and mode shapes of the plate, and compares one of these with the results obtained by a traditional experimental procedure.

DSTO ARL

MELBOURNE

CONTENTS

1   INTRODUCTION

In preparation for an experimental evaluation of the photogrammetry method for mode shape measurement, a steel specimen consisting essentially of a cantilevered plate, welded along one edge to a supporting member, was required. To provide a rigorous test of the photogrammetry technique, the cantilevered plate was required to be about one metre square, the modal amplitude to have a maximum value of ± 1.5 mm and the natural frequency of a multi-node mode to be about 25 Hz. This report describes the theory used to determine the plate dimensions, and gives a comparison of the theoretical mode shape with that measured by traditional methods. In a subsequent report this measured mode shape will be further compared with the one obtained by photogrammetry.

2   THEORETICAL ANALYSIS

Assuming that the supporting structure is rigid, the problem reduces to the analysis of a steel plate built in along one edge, with the other three edges free. Reference 1 provides simple formulae for calculating the natural frequencies and mode shapes of the first five modes of a square plate supported in this way. The modal amplitude may then be calculated from the known input force and the assumed value for the damping coefficient of the material. The fourth mode was selected and, in order to give the desired natural frequency, the thickness of the plate was set at three millimetres. One metre square steel plate was not available in this thickness so the specimen was made 1022 mm by 902 mm, with the shorter side being built in.

However since the plate is now not square the simplified formulae of Reference 1 no longer strictly apply and the appropriate mode shapes and natural frequencies were calculated in the following manner.

2.1   Modal Functions

Figure 1 shows the coordinate system for the cantilevered plate. Define two non-dimensional coordinates ξ and η as follows

$$\xi = x/a , \qquad \eta = y/b \qquad (1)$$

where a and 2b are the lengths of the free and fixed edge respectively. Following Reference 1, the plate mode shape is expanded in terms of beam

functions. These beam functions satisfy the beam boundary conditions corresponding to the free and clamped edges but their product does not satisfy the plate boundary conditions exactly.

In the x direction define the function

$$\varphi_i(\xi) = a_{1i}(\cosh \alpha_i\xi - \cos \alpha_i\xi) + b_{1i}(\sinh \alpha_i\xi - \sin \alpha_i\xi) \tag{2}$$

where α_i, the spatial frequency, is the i'th root of the non-linear equation

$$\cos\alpha \cosh\alpha = -1 \tag{3}$$

(See Appendix A for discussion on the solution of this transcendental equation.) The coefficients a_{1i} and b_{1i} are then given by

$$a_{1i} = \frac{2(\cosh\alpha_i + \cos\alpha_i)}{(1-e^{-\alpha_i})[e^{\alpha_i}(1+2\sin\alpha_i) + \cos\alpha_i - \sin\alpha_i]} \tag{4}$$

$$b_{1i} = \frac{2(-\sinh\alpha_i + \sin\alpha_i)}{(1-e^{-\alpha_i})[e^{\alpha_i}(1+2\sin\alpha_i) + \cos\alpha_i - \sin\alpha_i]} \tag{5}$$

The plate is symmetric about the x axis, so the modal functions in the y direction are separated into symmetric and antisymmetric groups. The antisymmetric functions ψ_a are defined by

$$\psi_{aj}(\eta) = a_{2j} \sinh \beta_j\eta + b_{2j} \sin \beta_j\eta \tag{6}$$

where the spatial frequency β_j is the j'th root of the equation

$$\tan \beta = \tanh \beta \tag{7}$$

and

$$a_{2j} = \frac{\cos\beta_j}{\cos\beta_j \sinh\beta_j + \sin\beta_j \cosh\beta_j} \tag{8}$$

$$b_{2j} = \frac{\cosh\beta_j}{\cos\beta_j \sinh\beta_j + \sin\beta_j \cosh\beta_j} \tag{9}$$

Equation 7 has a zero root (j=1) and the corresponding modal function is determined from l'Hopital's Rule to be

$$\psi_{a1}(\eta) = \eta \tag{10}$$

2

The corresponding symmetric functions are

$$\psi_{sj}(\eta) = a_{3j} \cosh \gamma_j\eta + b_{3j} \cos \gamma_j\eta \qquad (11)$$

where γ_j is the j'th root of

$$\tan \gamma = -\tanh \gamma \qquad (12)$$

and

$$a_{3j} = \frac{1}{2\cosh\gamma_j} \qquad (13)$$

$$b_{3j} = \frac{1}{2\cos\gamma_j} \qquad (14)$$

Equation 12 also has a zero root, and the corresponding modal function is then simply

$$\psi_{s1}(\eta) = 1 \qquad (15)$$

(See Appendix A for a discussion on the solution of equations 3, 7 and 12.)

A general mode of vibration may then be represented by the following bi-orthogonal expansion.

$$W(\xi,\eta) = \sum_{i=1}^{\infty}\sum_{j=1}^{\infty} \{ M_{ij} \varphi_i(\xi) \psi_{aj}(\eta) + N_{ij} \varphi_i(\xi) \psi_{sj}(\eta) \} \qquad (16)$$

where $W(\xi,\eta)$ is a normal mode. Since the plate is homogeneous and of uniform thickness all the normal modes of the plate are either exactly symmetric or antisymmetric about the x (or ξ) axis. That is, for any one mode $W(\xi,\eta)$ then for all i,j either $M_{ij} = 0$ or $N_{ij} = 0$. In this case the mode of interest is symmetric so equation 16 may be simplified to

$$W(\xi,\eta) = \sum_{i=1}^{\infty}\sum_{j=1}^{\infty} N_{ij} \varphi_i(\xi) \psi_{sj}(\eta) \qquad (17)$$

The set of modal functions used is of course not infinite but is truncated. In this case equation 17 becomes

$$W(\xi,\eta) = \sum_{i=1}^{n}\sum_{j=1}^{m} N_{ij} \varphi_i(\xi) \psi_{sj}(\eta) \qquad (18)$$

3

2.2 Plate Equation Of Motion

As stated in Reference 1, the classical equation of motion for plate dynamics is

$$D\nabla^4 w + \sigma \frac{\partial^2 w}{\partial t^2} = 0 \qquad (19)$$

where

$$D = \frac{Eh^3}{12\,(1-v^2)}$$

v is Poisson's ratio, σ is the plate area density, ∇^2 is the Laplacian operator, E is Young's modulus, h is the plate thickness and $w(\xi,\eta,t)$ is the plate transverse motion.

$$\nabla^2 = \frac{\partial^2}{\partial x^2} + \frac{\partial^2}{\partial y^2}$$

$$= \frac{1}{a^2}\frac{\partial^2}{\partial\xi^2} + \frac{1}{b^2}\frac{\partial^2}{\partial\eta^2} \qquad (20)$$

$$\therefore \quad \nabla^4 = \frac{1}{a^4}\frac{\partial^4}{\partial\xi^4} + \frac{2}{a^2 b^2}\frac{\partial^4}{\partial\xi^2\partial\eta^2} + \frac{1}{b^4}\frac{\partial^4}{\partial\eta^4} \qquad (21)$$

For sinusoidal motion we may write

$$w(\xi,\eta,t) = W(\xi,\eta)\,e^{i\omega t} \qquad (22)$$

Substituting this into equation 19 leads to

$$(D\nabla^4 - \omega^2\sigma)W = 0 \qquad (23)$$

which is a single scalar equation with unknowns N_{ij} and ω. If the functions φ and ψ satisfied all the plate boundary conditions then Galerkin's method could be used to transform this scalar equation into an eigenvalue equation, with the eigenvalues giving ω and the elements of each eigenvector being the corresponding values of N_{ij}. But the products $\varphi\psi$ satisfy only the geometric (clamped edge) boundary conditions, so the Rayleigh-Ritz method which gives solutions that inherently satisfy the natural (free edges) boundary conditions is used. This provides estimates of the first p ($p \leq nm$) natural frequencies and mode shapes, with the lower order modes being better estimated than the higher (due to truncation effects).

4

The shaker has a low armature mass (230 grams) and its natural frequency is approximately that of the mode of interest, so the effect of the shaker on the relevant natural frequency and mode shape is minimal. The calculated mode shape is shown in terms of its contours in Figure 2.

3 EXPERIMENTAL MEASUREMENT

The structural damping in the plate is sufficiently low (approximately 0.1%) for a normal mode to be excited with a single shaker, provided the excitation is not at a nodal line. An array of measuring stations was mapped out on the plate (Figure 3) which was then excited sinusoidally at 27.2 Hz to produce the required mode. A travelling accelerometer was used to measure the modal displacements at these points, and the beam functions of the previous section were fitted by a least squares process to these displacements to produce the contours shown in Figure 4. Note that both the symmetric and antisymmetric ψ functions were utilised to allow for possible asymmetry of the plate. (See Appendix B for a more general interpolation scheme.)

4 DISCUSSION

The natural frequency of the mode of interest was calculated to be 23.6 Hz whilst the measured natural frequency was 27.2 Hz. The free shaker has a natural frequency of 25 Hz and was attached to the plate at a point of relatively low amplitude in this mode, so it is not responsible for the frequency discrepancy. Also it is extremely difficult to build a plate which is truely "built in" along one edge as there is nearly always some motion at this edge. This should have led to the theoretical procedure overestimating the natural frequency rather than underestimating it. The plate was tested in the horizontal position which gave rise to a static deflection of about 66 mm along the free edge. Also it was welded to the mounting along the "built in" edge which distorted the plate somewhat such that it was no longer planar and this, coupled with the curvature resulting from the static deflection, gives rise to a greater stiffness than that of a flat plate.

The natural frequency of this mode (as of the other modes of the plate) is dependent on both the overall size of the plate and its aspect ratio (the ratio of a to 2b in Figure 1). If, due to non-planar distortion of the plate near the clamped edge, the "effective" length of

5

the cantilever were reduced, the fourth natural frequency would rise, giving better agreement with experiment. For example, if "a" were reduced by 20%, the natural frequency of this mode would rise by about 11%.

The two mode shapes are displayed in Figures 2 and 4. The latter figure shows that the excited mode is not symmetric about the x axis confirming the non-uniformity of the plate. Despite this, the main region of difference between the two sets of contours is in the area of the clamped edge. In Figure 2 the nodal lines run from the right hand (free) edge to the left hand (clamped) edge whereas in Figure 4 the nodal lines converge before reaching the clamped edge. The region of difference is one of small slope in this mode and small perturbations in amplitude result in significant changes in the contour pattern. The distortions of the plate cited above may also result in a non-uniformity of the stiffness distribution in this region. The correlation coefficient calculated between the two modes at the measurement points of Figure 3 is 0.946 which shows reasonable agreement.

5 CONCLUSION

Plate theory was used to design a specimen for use in a photogrammetry experiment. Following construction of the specimen, the natural frequency of the fourth mode was measured to be some 15% higher than that predicted. This may be may be due to the distortions introduced into the plate during fabrication and the static deformation of the plate under gravity. Although this classical plate theory was not adequate to predict accurately the dynamic behaviour of the distorted plate, the resultant natural frequency and mode shape of the test specimen satisfied the original requirements. i.e. to be suitable for the photogrammetry experiment.

6 REFERENCE

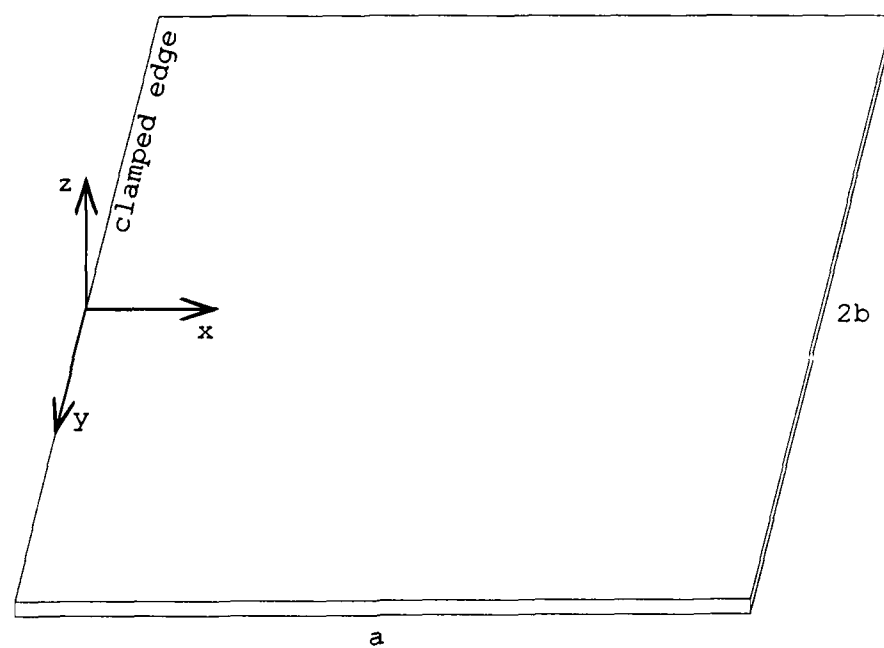1. Leissa A.,W. Vibration of Plates. NASA SP-160 1969.

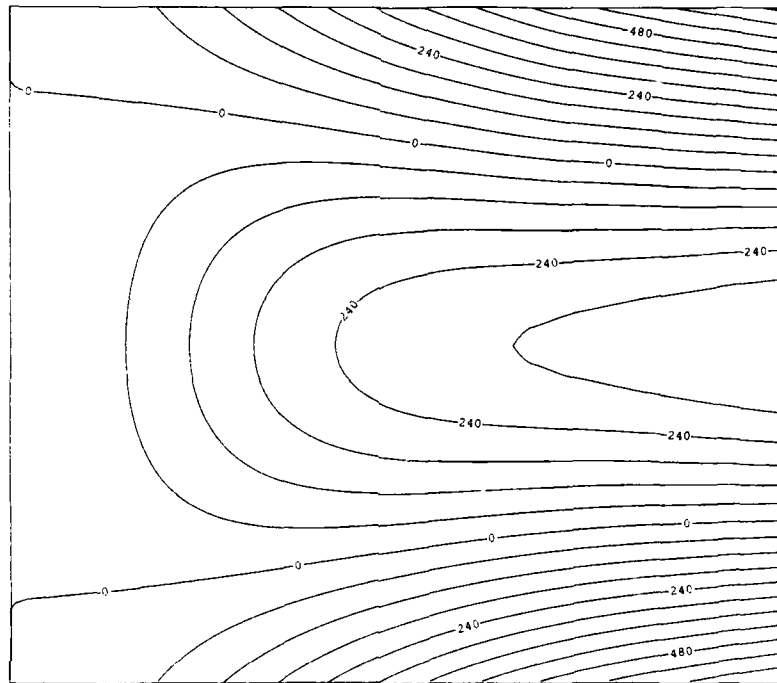*Figure 1. Rectangular cantilever plate, showing axis system*

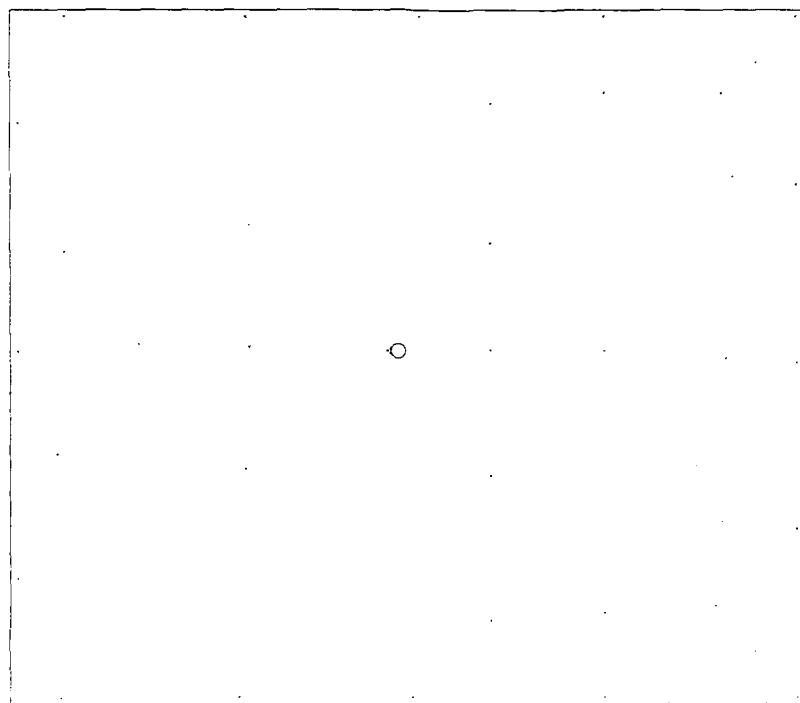*Figure 2. Contours depicting calculated mode shape*

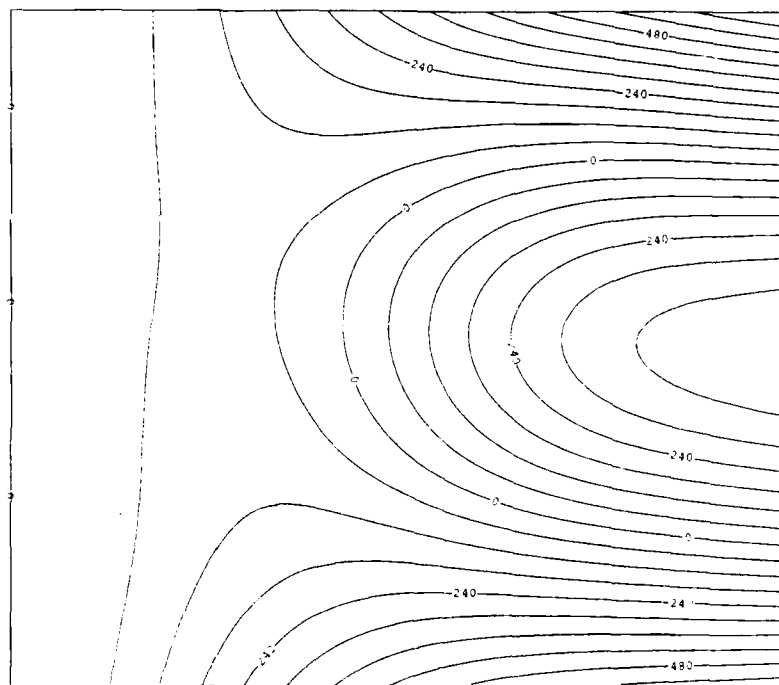*Figure 3. Location of measuring points, X, and shaker, O.*

Figure 4. Contours depicting measured mode shape

APPENDIX A

The three transcendental equations (3, 7 and 12) given in Section 2.1 must be solved for the spatial frequencies α , β and γ . This is done by using the Newton-Raphson method with initial estimates suitable to ensure a rapid rate of convergence.

A sufficient condition for the Newton-Raphson procedure to converge to a root of the equation

$$F(X) = 0 \tag{A-1}$$

is given by the total stability theorem. That is, we may linearise the equation

$$X_{n+1} = X_n - F(X_n)/F'(X_n) \tag{A-2}$$

about X_∞ and obtain

$$\delta X_{n+1} = \delta X_n - \frac{F'(X_n)\,\delta X_n}{F'(X_n)} + \frac{F(X_n)\,F''(X_n)\,\delta X_n}{(F'(X_n))^2} + HOT$$

$$= \frac{F(X_n)\,F''(X_n)\,\delta X_n}{(F'(X_n))^2} + HOT \tag{A-3}$$

where HOT indicates higher order terms. Provided that HOT is bounded, then the Newton-Raphson method will converge if

$$\left|\frac{F(X_n)\,F''(X_n)}{(F'(X_n))^2}\right| < 1 . \tag{A-4}$$

A-1

Furthermore, the non-dimensional function

$$\rho(X_n) = \left| \frac{F(X_n) F''(X_n)}{(F'(X_n))^2} \right| \qquad \text{(A-5)}$$

measures the exponential rate of convergence of the n'th estimate, X_n, towards the the correct value. For initial estimates, X_0, "sufficiently close" to a root of equation A-1, the rate of convergence after n iterations, as indicated by $\rho(X_n)$, will be be at least as fast as that indicated by $\rho(X_0)$. That is,

$$\rho(X_n) \le \rho(X_0)$$

Consider firstly equation 3 of Section 2.1. This may be written as

$$F(\alpha) = \cos\alpha \, \cosh\alpha + 1 = 0 \qquad \text{(A-6)}$$

$$\therefore F'(\alpha) = -\sin\alpha \, \cosh\alpha + \cos\alpha \, \sinh\alpha$$

and $F''(\alpha) = -2\sin(\alpha) \, \sinh(\alpha)$

$$\therefore \rho(\alpha) = \left| \frac{(\cos\alpha \, \cosh\alpha + 1)(-2\sin\alpha \, \sinh\alpha)}{(-\sin\alpha \, \cosh\alpha + \cos\alpha \, \sinh\alpha)^2} \right| \qquad \text{(A-7)}$$

Rewrite equation A-6 as

$$\cos\alpha = -1/\cosh\alpha$$

then as $\alpha \to \infty$, $\cos\alpha \approx 0$. Thus for initial estimates take

$$\alpha_{0i} = (2i-1)\pi/2 \qquad\qquad i=1,2,3\ldots\ldots \qquad \text{(A-8)}$$

Substituting these into equation A-7 gives

$$\rho(\alpha_{01}) = 0.731$$
$$\rho(\alpha_{02}) = 0.0359$$
$$\rho(\alpha_{03}) = 0.0016$$

For larger values of i, $\rho(\alpha_{0i}) \to 4e^{-\alpha}$.

A-2

Note that after two iterations these three convergence factors become

$$\rho(\alpha_{21}) = 0.0087$$
$$\rho(\alpha_{22}) = 0.23 \times 10^{-6}$$
$$\rho(\alpha_{23}) = 0.7 \times 10^{-12}$$

This indicates that convergence is rapid.

Similarly equation 7 may be written as

$$G(\beta) = \tan\beta - \tanh\beta = 0 \qquad \text{(A-9)}$$

$$\therefore \quad G'(\beta) = \tan^2\beta + \tanh^2\beta$$

and $\quad G''(\beta) = 2(\tan\beta + \tanh\beta + \tan^3\beta - \tanh^3\beta)$

The convergence function is again

$$\rho(\beta) = \left| \frac{G(\beta)\ G''(\beta)}{(G'(\beta))^2} \right| \qquad \text{(A-10)}$$

and the initial estimates are given by

$$\beta_{0j} = (4j-3)\pi/4 \qquad j=2,3,4.\ldots \qquad \text{(A-11)}$$

Note that the first root of equation A-9 is $\beta = 0$, so this is not obtained by iteration, and the corresponding modal function is

$$\Psi_{a1}(\eta) = \eta$$

Substituting the initial estimates (j=2,3,4..) into equation A-10 gives

$$\rho(\beta_{02}) = 0.78 \times 10^{-3}$$
$$\rho(\beta_{03}) = 0.14 \times 10^{-5}$$
$$\rho(\beta_{04}) = 0.27 \times 10^{-8}$$

For higher values of j, $\rho(\beta_{0j}) \to 2e^{-2\beta}$, again showing that convergence is rapid.

The symmetric functions from Section 2.1 lead to similar expressions. In this case the initial estimates are given by

$$\gamma_{0j} = (4j-5)\pi/4 \qquad j=2,3,4.\ldots \qquad \text{(A-12)}$$

where again the first root is $\gamma = 0$, and the corresponding modal function is

$$\psi_{s1}(\eta) = 1$$

The corresponding convergence factors are

$$\rho(\gamma_{02}) = 0.018$$
$$\rho(\gamma_{03}) = 0.34 \times 10^{-4}$$
$$\rho(\gamma_{04}) = 0.63 \times 10^{-7}$$

and, as before, $\rho(\gamma_{0j}) \rightarrow 2e^{-2\gamma}$ for larger values of j, showing rapid convergence.

APPENDIX B

As described in Section 3, beam functions with the correct boundary conditions were used to interpolate the measured modal displacements to sufficient other locations on the plate to produce the contours shown in Figure 4. A more general interpolation technique which is not constrained by particular edge conditions but which fits a surface of minimum curvature to the measured mode shape may be used.

The equation which gives the displacement of an infinite plate subjected to a number (n) of point loads is

$$w(x,y) = a + bx + cy + \sum_{i=1}^{n} f_i\, r_i^2\, \log(r_i) \qquad (B-1)$$

where $r_i^2 = ((x-x_i)^2 + (y-y_i)^2)$

and f_i is the point load applied at the point (x_i,y_i).

This same equation results from the solution to the problem of fitting a surface of minimum curvature with the constraint that it pass through n points (x_i,y_i,w_i) where (x_i,y_i) are the coordinates of the i'th measurement point and w_i is the measured modal amplitude at this point.

Equation B-1 may be evaluated at the n measurement points, leading to n simultaneous equations in the n+3 unknowns $a,b,c,f_1,\ldots,f_n$. The three extra equations result from the equilibrium conditions

$$\sum_{i=1}^{n} f_i = 0 \qquad (B-2)$$

$$\sum_{i=1}^{n} f_i x_i = 0 \qquad (B-3)$$

$$\sum_{i=1}^{n} f_i y_i = 0 \qquad (B-4)$$

Note that these last three equations are independent of the measured displacements, w_i.

Ordering these equations in the sequence B-2, B-3, B-4 and then the n equations resulting from B-1, we may express the resulting n+3 simultaneous equations in matrix form as

$$U = J V \qquad (B-5)$$

where U is the vector of elements $0,0,0,w_1,\ldots,w_n$
    V is the vector of elements $a,b,c,f_1,\ldots,f_n$,
  and J is a symmetric matrix.

For non-trivial solutions J may be inverted to give

$$V = J^{-1} U \qquad (B-6)$$

Because the first three elements of U are zero the matrix J^{-1} may be partitioned after the first three rows and columns, and the lower right n × n submatrix extracted to give

$$F = K W \qquad (B-7)$$

where F is the vector of elements $f_1,\ldots,f_n$,
    W is the vector of elements $w_1,\ldots,w_n$,
  and K is a symmetric submatrix of J^{-1}.

Thus equation B-6 may be solved for the coefficients in Equation B-1 and the mode shape evaluated everywhere on the plate. However this surface is constrained to pass exactly through the measured mode shape displacements which are subject to measurement noise. Consequently it is better to formulate the solution in terms of a "relaxed" least squares problem subject to a constraint.

Returning to the analogy of the plate acting under point loads, the work done in applying these loads is

$$\text{work} = F^T W \qquad (B-8)$$

where the superscript T indicates transposition.
The work done equals the increase in potential energy of the deformed plate and this in turn is related to the curvature of the plate. So to minimise the curvature we may minimise the work. Thus the problem becomes:

Minimise $F^T W$

subject to the constraint

$$[W-W^*]^T [W-W^*] = n \sigma^2$$

where F is the vector of n coefficients f_i,
    W^* is the vector of "noisy" measured displacements,
    W is the vector of "true" displacements (i.e. without measurement noise)
  and σ^2 is the variance of the measurement noise.

Using Lagrange multipliers this may be written as

$$0.5 \ F^T W + 0.5 \ \lambda \ [W-W^*]^T \ [W-W^*] = E \tag{B-9}$$

Substituting Equation B-7 into Equation B-9 gives

$$0.5 \ W^T K W + 0.5 \ \lambda \ [W-W^*]^T \ [W-W^*] = E \tag{B-10}$$

Application of the Variational Principle gives

$$[K + \lambda I] \ W = \lambda \ W^* \tag{B-11}$$

where I is the unit matrix.

$$\text{Put } \varepsilon = 1/\lambda \tag{B-12}$$

Then Equation B-11 becomes

$$[I + \varepsilon K] \ W = W^* \tag{B-13}$$

It is then required to find the unique ε such that the vector W obtained from equation B-13 satisfies the equation

$$[W-W^*]^T \ [W-W^*] - n \sigma^2 = 0 \tag{B-14}$$

This may be done by iteration with the initial value of ε being

$$\varepsilon_{INITIAL} = \text{Trace}(K) \tag{B-15}$$

In the present case (a cantilever plate) the edge conditions are well stated and the corresponding beam functions have already been determined for the theoretical analysis of Section 2. Consequently these beam functions are best used for interpolation here. However in a

more general problem the necessary beam functions may not be readily available and the application of the approach in this appendix may be useful.

DISTRIBUTION

AUSTRALIA

Department of Defence

Defence Central
Chief Defence Scientist
AS, Science Corporate Management (shared copy)
FAS Science Policy (shared copy)
Director, Departmental Publications
Counsellor, Defence Science, London (Doc Data Sheet Only)
Counsellor, Defence Science, Washington (Doc Data Sheet Only)
OIC TRS, Defence Central Library
Document Exchange Centre, DSTIC (18 copies)
Joint Intelligence Organisation
Librarian H Block, Victoria Barracks, Melbourne

Aeronautical Research Laboratory
Director
Library
Divisional File Aircraft Structures
Authors: P.A. Farrell
T. Ryall
B. Emslie
A. Goldman

Materials Research Laboratory
Director/Library

Defence Science & Technology Organisation - Salisbury
Library

WSRL
Maritime Systems Division (Sydney)

Air Force Office
Air Force Scientific Adviser (Doc Data sheet only)
Aircraft Research and Development Unit
Scientific Flight Group
Library
Engineering Branch Library
Director General Engineering - Air Force

Universities and Colleges

LaTrobe
Library

Melbourne
Engineering Library
Dr M. Shortis, Department of Surveying

Monash
Hargrave Library
Head, Materials Engineering

Newcastle
Library
Professor R. Telfer, Institute of Aviation

Sydney
Engineering Library
Head, School of Civil Engineering

NSW
Physical Sciences Library
Head, Mechanical Engineering
Head, Fuel Technology
Library, Australian Defence Force Academy

RMIT
Library
Mr M.L. Scott, Aerospace Engineering
Mathematics Department
Dr G. Fitz-Gerald
Dr J. Gear

SPARES (10 COPIES)

TOTAL (64 COPIES)

AL 149   DEPARTMENT OF DEFENCE

DOCUMENT CONTROL DATA

PAGE CLASSIFICATION
UNCLASSIFIED
PRIVACY MARKING

1a. AR NUMBER AR-006-120	1b. ESTABLISHMENT NUMBER ARL-STRUC-TM-568	2. DOCUMENT DATE JULY 1990	3. TASK NUMBER DST 90/033

4. TITLE VIBRATION OF A RECTANGULAR CANTILEVER PLATE	5. SECURITY CLASSIFICATION (PLACE APPROPRIATE CLASSIFICATION IN BOX(S) IE. SECRET (S), CONF. (C) RESTRICTED (R), UNCLASSIFIED (U)). U U U DOCUMENT TITLE ABSTRACT	6. NO. PAGES 20 7. NO. REFS. 1

8. AUTHOR(S) P.A. Farrell T.G. Ryall	9. DOWNGRADING/DELIMITING INSTRUCTIONS Not applicable

10. CORPORATE AUTHOR AND ADDRESS **AERONAUTICAL RESEARCH LABORATORY** **P.O. BOX 4331, MELBOURNE VIC 3001**	11. OFFICE/POSITION RESPONSIBLE FOR: SPONSOR _____ DSTO _____ SECURITY _____-_____ DOWNGRADING _____-_____ APPROVAL _____ CSTD _____

12. SECONDARY DISTRIBUTION (OF THIS DOCUMENT) Approved for public release OVERSEAS ENQUIRIES OUTSIDE STATED LIMITATIONS SHOULD BE REFERRED THROUGH DSTIC, ADMINISTRATIVE SERVICES BRANCH, DEPARTMENT OF DEFENCE, ANZAC PARK WEST OFFICES, ACT 2601

13a. THIS DOCUMENT MAY BE ANNOUNCED IN CATALOGUES AND AWARENESS SERVICES AVAILABLE TO . . . . No limitations

13b. CITATION FOR OTHER PURPOSES (IE. CASUAL ANNOUNCEMENT) MAY BE	X UNRESTRICTED OR	☐ AS FOR 13a.

14. DESCRIPTORS Photogrammetry Vibration measurement Vibration mode	15. DISCAT SUBJECT CATEGORIES 2011

16. ABSTRACT

In preparation for an experimental evaluation of the photogrammetry technique for measuring vibration mode shapes, a cantilever steel plate was designed. This report describes the theoretical methods used to calculate the low order natural frequencies and mode shapes of the plate, and compares one of these with the results obtained by a traditional experimental procedure.

THIS PAGE IS TO BE USED TO RECORD INFORMATION WHICH IS REQUIRED BY THE ESTABLISHMENT FOR ITS OWN USE BUT WHICH WILL NOT BE ADDED TO THE DISTIS DATA UNLESS SPECIFICALLY REQUESTED.

16. ABSTRACT (CONT).

17. IMPRINT

AERONAUTICAL RESEARCH LABORATORY, MELBOURNE

18. DOCUMENT SERIES AND NUMBER	19. COST CODE	20. TYPE OF REPORT AND PERIOD COVERED
Aircraft Structures Technical Memorandum 568	23 2110	

21. COMPUTER PROGRAMS USED

22. ESTABLISHMENT FILE REF.(S)

23. ADDITIONAL INFORMATION (AS REQUIRED)